Annual Status Report

For the Period: December 15, 1993 - December 14, 1994

Under NASA Grant No. NAG3-1381, Basic

NASA Technical Officer: Dr. Subush Jayawardena and Dr. Bhin Singh

REWETTING OF MONOGROOVE HEAT PIPE IN SPACE STATION RADIATORS

by

S.H. Chan

Wisconsin Distinguished Professor
Department of Mechanical Engineering
University of Wisconsin-Milwaukee
Milwaukee, Wisconsin 53201

Prepared for

NASA

Lewis Research Center
21000 Brookpark Road
Cleveland, OH 44135

ABSTRACT

This annual report summarizes the work accomplished on rewetting of monogroove heat pipe in space station. Specifically, theoretical and experimental investigations of the rewetting characteristics of thin liquid films over unheated and heated capillary grooved plates were performed. To investigate the effect of gravity on rewetting, the grooved surface was placed in upward and downward facing positions. Profound gravitational effects were observed as the rewetting velocity was found to be higher in the upward than in the downward facing orientation. The difference was even greater with higher initial plate temperatures. With either orientation, it was found that the rewetting velocity increased with the initial plate temperature. But when the temperature was raised above a rewetting temperature, the rewetting velocity decreased with the initial plate temperature. Hydrodynamically controlled and heat conduction controlled rewetting models were then presented to explain and to predict the rewetting characteristics in these two distinct regions. The predicted rewetting velocities were found to be in good agreement with experimental data with elevated plate temperatures.

INTRODUCTION

Rewetting of the heated monogroove heat pipe is an important consideration in the design of space station radiators. When the thermal radiator is overloaded with a heat flux discharge from the condenser of the thermal bus system in the space station, dryout occurs on the circumferential section of the monogrooved heat pipe located directly underneath the heat flux. Therefore it is of interest to investigate the rewetting characteristics of liquid films on a heated plate with a grooved surface, which simulates the circumferential section of the monogrooved heat pipe.

The use of capillary grooved surfaces is of course not limited to the monogroove heat pipe. They are widely used in the thermal control of space- based applications and in the heat transfer enhancement of electronic devices. For space-based applications, it is imperative that the effects which gravitational variations have upon the capillary grooved surface be considered.

The rewetting process is a conjugated heat transfer problem involving interactions between a solid wall and a flowing fluid. The rewetting process of a heated grooved plate is quite complicated, as the rewetting velocity varies with time, groove geometry, plate and fluid properties and applied heat flux. Several investigations (Yamanouchi,1968; Thompson, 1972; Duffey and Porthouse, 1973; Sun et al., 1974; Alario et al., 1983; Grimley et al., 1988; Stroes et al., 1990; Ferng et al., 1991; Peng and Peterson, 1991 and 1992, Chan and Zhang, 1994) dealing with the rewetting characteristics of liquid films on heated rods, tubes and flat plates have been made. However, effects of gravity on the rewetting process of a capillary grooved surface have not been reported and a solution for the rewetting process of a finite length of heated smooth/grooved plate with the end of the plate maintained at an isothermal condition has not been

presented. Such a boundary condition is one of the possibilities that may apply to the circumferential section of the monogrooved heat pipe.

One objective is to investigate gravitational effects using simulation experiments at normal gravity. This was achieved by studying the rewetting of a heated and unheated plate with its grooved surface in upward and downward facing orientations. Another objective is to investigate, both experimentally and theoretically, the rewetting characteristics on grooved surfaces with an isothermal end condition under 1-g condition, and to present rewetting models which explain and predict the rewetting characteristics. Finally, the results of experimental investigations into other factors which effect the rewetting of the plate are reported.

REWETTING OF UNHEATED GROOVED PLATE

Experiment Experiments were first conducted at room temperature to study how the rewetting of an unheated, grooved plate was affected by variations in plate orientation and mass flow rate of working fluid supplied to the plate. The experimental setup at the room temperature condition consists of a liquid supply system with an adjustable flow rate, a test section (containing the grooved plate) and a video recording system with high resolution frame by frame playback capability. The working liquid (2-propanol) is delivered to the grooved plate (the test section) through an outwardly slanted slot of the coolant feeder as shown in Fig.1 to avoid imposing pressure or inertial force in the advancing direction of the liquid. Thus the motion of the liquid is mainly driven within the grooves by capillary force. The grooved plate is fashioned from a sheet of oxygen free copper. Following each experimental run, the grooved surface is cleaned with Oakite® and rinsed with distilled water. The grooved surface is then blown dry with compressed air. The groove geometry is shown

in Fig.1. Experimental runs are recorded with a Super-VHS-C camcorder. The tape is then played back on a S-VHS VCR frame by frame to determine the position of the liquid front vs time (1/30 second per frame)

Results and Discussion The liquid supply flow rate's effect on transient wicking length and wetting velocity are shown in Fig.2. Three flow rates were used: m = 15, 32 and 41 $^{ml}/_{min}$. The lowest flow rate was found to provide an inadequate amount of working fluid to rewet the plate. It was also found that at a higher flow rate (32 $^{ml}/_{min}$ or higher), increasing the flow rate had little effect on the rewetting of the plate as shown in Fig.2. After this finding, both the unheated and heated tests were performed at the flow rate of 38 $^{ml}/_{min}$. The comparison between the upward and downward facing cases (i.e. the horizontal grooved surface facing upward and downward respectively) at room temperature is shown in Fig.3 (the 22 C case). It was found that the rewetting distance, and therefore rewetting velocity, in the upward facing case is higher than that in the downward facing case. This is probably because the liquid in the groove is being pressed against the groove surface by gravity in the face up case, thus making a better contact than in the face down case where the liquid is pulled away from the groove surface. Another cause may be a slightly larger surface tension force in the face up case than that in the face down case. This was illustrated by placing the grooved plate in various inclinations with one end immersed in 2-propanol and unity oil respectively. It was found that for both fluids, the mean wicking lengths in the upward facing orientation were slightly larger than the downward facing, as shown in Fig.4. The figure also shows that an evaporating fluid (2-propanol) and a non evaporating fluid (unity oil) follow a similar trend. Thus the wicking length difference is attributed primarily to the plate orientation rather than evaporation. Such a

phenomenon may be attributed to differences in the effective contact angles when the plate is placed in different orientations.

REWETTING OF HEATED GROOVED PLATE

Experiment For the heated cases, the experimental apparatus consists of the following components (Fig.1): A liquid supply system with an adjustable flow rate, an experimental platform which contains a grooved plate with embedded thermocouples evenly spaced along the bottom in the groove direction, a data acquisition system with multiplexer to simultaneously read and record the signals from the thermocouples, a heater with a temperature controller for maintaining a constant heater temperature, a traveling thermocouple sensor used to measure temperatures along the top of the plate, a video recording system capable of recording and playing back high resolution pictures frame by frame, and a signal light to synchronize the computer data acquisition with the video.

The plate was chemically cleaned, and then heated at one end to the desired initial temperature. The video camera was activated, and a signal light was turned off to indicate the commencement of computer data acquisition. The working fluid was then introduced to the plate, and the rewetting process was recorded. If desired, surface temperatures were also measured using a traveling thermocouple. The traveling thermocouple was useful for determining the liquid-plate interface temperature of the liquid front, as well as for gauging the accuracy or serviceability of the embedded thermocouples. When working with 2-propanol, extreme care was taken to insure adequate insulation, ventilation and fire safety.

Rewetting experiments were conducted with the plates preheated to various initial temperatures and with plates in the face up and face down orientations.

Results and Discussion Experiments were performed at several plate temperatures in both the face up and face down orientations.

The format for the presentation of the experimental data is a contour plot of temperature reading as a function of thermocouple location and time of acquisition. The location of the fluid front, which was observed from video, is superimposed on the contour maps. Thermal resolution is ± 1 C, and is determined by the accuracy of the thermocouple. Temporal resolution is 0.5 sec., and is determined by the data acquisition rate. Spatial resolution is 0.5 cm, and is estimated from observation of the fluid front, which is not perfectly even in its advance.

To depict the effect of plate orientation (face up or face down), the heated plate case which is presented is one in which the initial plate temperature is above 110 C. The face down (Fig.5) and face up (Fig.6) orientations are compared. Following the fluid front for the face down case (Fig.5), it is seen that the front travels between 95 C and the 100 C contour lines (rewetting temperature contour lines). If allowed to continue, the front advances to around 82 mm in two minutes. It should be noted that during the face down (Fig.5) experiment, the thermocouples located at 92 mm malfunctioned. This resulted in the contour anomalies at the 92 mm position, and hence those temperature readings were edited from the data. For the face up case (Fig.6), the front follows between the 95 C and 100 C contour lines as well. If the fluid is allowed to continue, the front advances to around 120 mm in 2 minutes.

A comparison between Fig.5 and Fig.6 shows a significant difference in the temperature profiles, and that the rewetting is much slower in the downward facing than in the upward facing cases. They clearly indicate a possible gravitational effect on the heat transfer from the capillary grooved surface to liquids, which can only be tested by microgravity

experiments. The latter is being planned. While the microgravity data are currently unavailable for the rewetting of capillary grooved surfaces, references can be made to some existing microgravity data of other geometries. Lyon et al. (1956) provided reduced gravity critical heat flux (CHF) data for horizontal surfaces by using magnetic body force. It was found that if the magnetic force was increased sufficiently to provide a negative gravity to lift the liquid from the surface, the CHF decreased to very close to zero. Merte and Clark (1964) reported heat flux vs. surface temperature data for liquid nitrogen boiling on a copper sphere in a drop tower experiment. Their results showed that the CHF and film boiling heat transfer were significantly affected by gravity, though the nucleate boiling heat transfer was not. Kawaji and Westbye (1991) conducted two-phase flow and heat transfer experiments in microgravity by quenching a heated quartz tube and filling a vessel aboard NASA's KC-135. They also found that the heat transfer under the microgravity condition was substantially reduced. The above microgravity boiling data, though incomplete, can be used to help the explanation of the present rewetting data. For the face down case, the liquid is pulled away by gravity from the grooved bottom surface. Additionally, the bubbles or vapor layer formed tend to stay close to the heated surfaces as in reduced gravity. Therefore, the heat transfer is expected to decrease substantially, resulting in a smaller rewetting velocity and a significantly different temperature profile when compared to the face up case.

To depict the interdependence among the rewetting temperature, rewetting front velocity and the temperature profile of the plate, surface plots have been generated. Figures 6-8 show the results for the grooved plate facing upward at elevated initial temperatures. Fig.6 ($T_I \simeq 110$ C) shows the rewetting front temperature (rewetting temperature)

following the contour between 95 C and 100 C. Also observe that after 25 seconds the front had advanced to around 85 mm. In Fig.7 (T_i≃120 C) one can see the front following the 104 C contour line and progressing to around 65 mm in 25 seconds. And finally, looking at Fig.8 (T_i≃130 C) one sees that the front follows the 104 C contour line, but advances to only about 45 mm. It should also be noted that the initial transient period (the period in which the front position crosses the contour lines) increases with initial temperature. This period was around 8 seconds for T_i≃110 C and T_i≃120 C, and around 12 seconds for T_i≃130 C.

The measured transient rewetting distances on a heated grooved plate, with different initial plate temperatures are summarized in Fig.3. Comparing the 110 C and 22 C cases (Fig.3), reveals that the difference between the upward and the downward facing rewetting distances increases with plate temperature. It is also found that the rewetting distance increases with the initial plate temperature, but then decreases with the plate temperature when the latter exceeds the rewetting temperature. Rewetting models are presented next to explain this seemingly contradictory trend.

REWETTING MODELS AND COMPARISON BETWEEN PREDICTIONS AND EXPERIMENTS

In the rewetting process of monogroove heat pipe, it is important to predict the liquid advancing velocity. If the initial plate temperature is less than the rewetting (or equivalent Leidenfrost) temperature, the advancing liquid is believed to be hydrodynamically controlled, namely, governed by the balance of the capillary surface tension force, friction force, gravitational force and the acceleration term as described by

$$\frac{\sigma}{R}A_1=\tau_w A_w+mg\sin\alpha+m\frac{du}{dt} \qquad (1)$$

where R is the characteristic capillary radius, σ the surface tension, m the total mass of liquid in the grooves and in the reservoir entrance region (Levine et al., 1976 and Dreyer et al., 1994), A_l the liquid cross sectional area, α the inclination angle of the plate, u the liquid front mean velocity, A_w the wetted wall area, and $\tau_w=f\rho u^2/8$ shear stress where f is assumed to be equal to $64/Re_{Dh}$. The initial condition for the above equation is: u=0 when t=0.

To simplify the problem, R is assumed to be constant and equal to half of the groove width, which is equivalent to a contact angle of zero. From Fig.3, it can be seen that the predictions for the cases (22 C and 80 C in Fig.3) where the initial plate temperature is less than the rewetting temperature are in good agreement with the experimental data. For the face down case, the use of the same capillary radius or contact angle seems to slightly overestimate the driving force. Since the above experimental results (Fig.4) show that the mean wicking lengths of the unheated plate in the upward facing orientation are slightly larger than that in the downward facing orientation, the effective capillary radius or contact angle may be affected by plate orientation. Therefore, the value of the equivalent contact angle in the face down case was adjusted slightly upward accordingly. However, the difference in the prediction between the face up and the face down positions is still relatively insignificant, as shown in the 22 C case in Fig.3.

For the plate with initial temperatures above the rewetting temperature, the rewetting process is assumed to be conduction-controlled. This is based on the premise that the liquid front can advance only after the plate ahead of the front has been quenched down to a rewetting (Leidenfrost) temperature by the axial conduction in the plate. In keeping with a prior study (Chan and Zhang, 1994), the following assumptions are made: a constant averaged heat transfer

coefficient in the wet region to remove the heat from the thin plate to the liquid film, no heat loss to the environment in the dry region, the plate at the rewet front remains at a constant Leidenfrost temperature T_0 although the experiment shows that the rewet front temperatures change with time in the rewetting process, the liquid film remains at the saturation temperature T_s , and the plate is thin enough that a one-dimensional model can be used. The rewetting process is sketched in Fig.1. The governing equation is the same as the prior study on a plate with uniform heating from beneath (Chan and Zhang, 1994) except that

$$A=\frac{q(S_1-l_1)}{K(T_0-T_S)}=0$$

for lack of heating from beneath the plate (q = 0). With a Lagrangian Coordinate moving with the rewetting front, the governing equation in the wet region ($-\eta_{L1}<\eta<0$) is as follows:

$$\frac{\partial\theta}{\partial\tau}=\frac{\partial^2\theta}{\partial\eta^2}+P\frac{\partial\theta}{\partial\eta}-B\theta \qquad (2)$$

where

$$P=\frac{V(S_1-l_1)\rho C_P}{K}; \qquad B=\frac{h(S_1-l_1)}{K}$$

$$\theta(\eta,\tau)=\frac{T-T_S}{T_0-T_S}; \qquad \eta=\frac{X}{(S_1-l_1)} \qquad (3)$$

$$\tau=\frac{t}{[(S_1-l_1)^2\rho C_P/K]}$$

In the above, B is the Biot number; P, $\theta(\eta,\tau)$, η, τ are the dimensionless rewetting velocity (Peclet number), temperature, length and time, respectively. The same equation with B=0 can be used for the dry region ($0<\eta<\eta_{L2}$).

The initial condition is

$$\theta(\eta,0)=\frac{T_1-T_S}{T_0-T_S}=\theta_1 \tag{4}$$

where T_1 is the initial hot surface temperature, while the boundary conditions are

$$\theta(-\eta_{L_1},\tau)=0$$

$$\theta(0,\tau)=1 \tag{5}$$

$$\theta(\eta_{L_2},\tau)=\theta_1$$

An approximate, analytical solution for eq.(2) can be found by assuming a constant initial surface temperature, and by treating the Peclet number, P, as a constant value in the mathematical deliberation in order to achieve a closed form solution. By setting the dimensionless heat source equal to zero (A=0) in the previous solution for the uniform heating (Chan and Zhang, 1994), the approximate analytical solution of eq.(2) is

$$\theta(\eta,\tau)=\frac{e^{(r_2\eta-r_1\eta_{L_1})}-e^{(r_1\eta-r_2\eta_{L_1})}}{e^{-r_1\eta_{L_1}}-e^{-r_2\eta_{L_1}}}+e^{\alpha_1\eta+\beta_1\tau}\sum_{n=1}^{\infty}a_{n_1}\sin\left[-\frac{n\pi\eta}{\eta_{L_1}}\right]e^{\frac{-n^2\pi^2\tau}{\eta_{L_1}^2}} \tag{6}$$

for the wet region and

$$\theta(\eta,\tau)=e^{\alpha_2\eta+\beta_2\tau}\left[\sum_{n=1}^{\infty}a_{n_2}\sin\left[\frac{n\pi\eta}{\eta_{L_2}}\right]e^{-\frac{n^2\pi^2\tau}{\eta_{L_2}^2}}\right]+1-\left(\frac{\theta_1-1}{e^{-P\eta_{L_2}}-1}\right)(1-e^{-P\eta}) \quad (7)$$

for the dry region. The dimensionless rewetting velocity, P, is given by:

$$-\frac{P}{2}+\sqrt{P^2+4B}\left[\frac{1}{2}-\frac{1}{1-e^{(r_1-r_2)\eta_{L_1}}}\right]-\sum_{n=1}^{\infty}\left[\frac{n\pi}{\eta_{L_1}}a_{n_1}e^{\beta_1\tau-\frac{n^2\pi^2\tau}{\eta_{L_1}^2}}+\frac{n\pi}{\eta_{L_2}}a_{n_2}e^{\beta_2\tau-\frac{n^2\pi^2\tau}{\eta_{L_2}^2}}\right]$$

$$+P\frac{\theta_1-1}{e^{-P\eta_L}-1}=0 \quad (8)$$

where

$$r_1=\frac{-P+\sqrt{P^2+4B}}{2};\qquad r_2=\frac{-P-\sqrt{P^2+4B}}{2}$$

$$\alpha_1=-\frac{P}{2};\qquad \beta_1=-B-\frac{P^2}{4}$$

$$a_{n_1}=-\frac{2}{\eta_{L_1}}\int_{-\eta_{L_1}}^{0}f_1(v)\sin\left[\frac{-n\pi v}{\eta_{L_1}}\right]dv$$

$$f_1(v)=e^{-\alpha_1 v}\left\{\theta_1-\left[1-\frac{e^{-r_1\eta_{L_1}}}{e^{-r_1\eta_{L_1}}-e^{-r_2\eta_{L_1}}}\right]e^{r_1 v}-\left[\frac{e^{-r_1\eta_{L_1}}}{e^{-r_1\eta_{L_1}}-e^{-r_2\eta_{L_1}}}\right]e^{r_2 v}\right\} \quad (9)$$

$$\alpha_2=-\frac{P}{2};\qquad \beta_2=-\frac{P^2}{4}$$

$$a_{n_2}=\frac{2}{\eta_{L_2}}\int_{0}^{\eta_{L_2}}f_2(w)\sin\left[\frac{n\pi w}{\eta_{L_2}}\right]dw$$

$$f_2(w) = \{\theta_1 - [(1 - \frac{\theta_1 - 1}{e^{-P\eta_{L_2}} - 1}) + (\frac{\theta_1 - 1}{e^{-P\eta_{L_2}} - 1}) e^{-Pw}]\} e^{-\alpha_2 w}$$

For the initial temperature of 110 C, the analytical solution using above equations are illustrated in Fig.9.

Also shown in the figure are the numerical solutions obtained by solving for the following alternative governing equation fixed in the nonmoving coordinates (η',t) as sketched in Fig.1:

$$\frac{\partial\theta}{\partial\tau} = \frac{\partial^2\theta}{\partial\eta'^2} - B\theta \qquad (10)$$

with the same assumptions as that of eq.(2). By using the variable space method (Murray and Landis, 1959) to deal with the moving-boundary problem, eq.(10) becomes:

$$\frac{d\theta_n}{d\tau} = \frac{\partial\theta_n}{\partial\eta'}\frac{d\eta_{L_1}}{d\tau}\frac{\eta'_n}{\eta_{L_1}} + \frac{\partial^2\theta_n}{\partial\eta'^2} - B\theta_n \qquad for \quad 0<\eta'<\eta_{L_1} \ ;$$

$$\frac{d\theta_n}{d\tau} = \frac{\partial\theta_n}{\partial\eta'}\frac{d\eta_{L_1}}{d\tau}\frac{\eta_L - \eta'_n}{\eta_L - \eta_{L_1}} + \frac{\partial^2\theta_n}{\partial\eta'^2} \qquad for \quad \eta_{L_1}<\eta'<\eta_L \qquad (11)$$

where subscript n denotes n-th grid point, and η_{L1} is a non-dimensional distance of the liquid front determined by matching the following condition:

$$\frac{\partial\theta}{\partial\eta'}\Big|_{dry} = \frac{\partial\theta}{\partial\eta'}\Big|_{wet} \qquad (12)$$

Numerical calculation of eq(10) was performed simultaneously for both the wet and dry regions. In order to see whether the approximate analytical form solution is close to the numerical

solution, numerical calculation has been performed using the same conditions as the analytical calculation and it is found that the difference is almost nondiscernable in the ranges of most interest, as shown in Fig.9.

From the calculation it was found that the heat conduction controlled model is sensitive to the value of the rewetting temperature, namely plate temperature at the liquid front. An increase in temperature of the liquid front by a few degrees led to a significant increase in the calculated liquid front velocity. From the experiment, the rewetting temperature was found to vary with the initial temperature and the liquid front location (time), in a range between 95 C and 104 C. Therefore the constant rewetting temperature assumption at the liquid front, which is adopted in the current conduction controlled model, may need to be improved further. In the current calculation, a rewetting temperature value of 95 C was used to calculate the transient liquid advancing location and temperature profile. The numerical prediction of the rewetting distances and the plate axial temperature profiles are compared with experimental data in Fig.3 and Fig.10 respectively. In these numerical calculations, the measured initial temperature profiles of the plate were inputed as the initial condition, $\theta(\eta',0)$. In Fig 10(a) and (b), the end of the heated grooved plate was maintained at 120 C and 150 C respectively. The predicted transient plate temperature profiles generally agree well with the data as shown in Fig. 10, except near the liquid entrance region, where the plates don't seem to quench as quickly as predicted. Since the corresponding initial temperatures of the first 6 cm length of the plate (which is of interest in monogroove heat pipe application) are relatively isothermal at 110 C and 130 C respectively, these isothermal temperatures are used to label the data in Fig.3. In Fig.3, many more sets of data including the room temperature data are presented. As mentioned earlier, at a given time, the wet front penetration

distance increases with increasing initial plate temperature, and the trend is reversed as the plate temperature is raised above the rewetting temperature. The reverse trend clearly indicates that the mechanisms governing the rewetting process are different. For this reason, it prompts the present study to propose the hydrodynamic control rewetting model for cases where $T_1 < T_0$ and the conduction control model for $T_1 > T_0$. In the former, as T_1 increases, the friction term (more precisely the laminar viscosity μ) decreases much faster than the surface tension driven term (σ) since μ and σ vary approximately with temperature as:

$$\mu_{t_1}=\mu_{293}\left(\frac{T_1}{293}\right)^{m} \qquad where\ m=-7.425$$

$$\sigma_{T_1}=\sigma_{293}\left(\frac{T_1}{293}\right)^{n} \qquad where\ n=-1.032$$

for the range of experimental conditions here. Thus the rewetting velocity and rewetting distance predicted by eq.(1) increases with T_1 as can be seen in Fig.3 by comparing the case of T_1 = 22 C with T_1 = 80 C. On the other hand, for $T_1 > T_0$ (which is taken as 95 C), the predicted rewetting distance, and therefore the predicted rewetting velocity, by the conduction control model decrease with increasing T_1, which is also in agreement with the data. This is because when the plate initial temperature is maintained at a temperature higher than the rewetting temperature T_0, the plate temperature ahead of the wetting front (i.e. in the dry region) has to be cooled down to the rewetting temperature by the axial conduction in the plate before the wetting front can advance further. As the initial plate temperature increases, more thermal heat capacity of the plate has to be removed by conduction, and thus a slower rewetting velocity and shorter rewetting distance can be expected.

CONCLUSION

This study reports results of experimental and theoretical investigations of the rewetting characteristics of a thin liquid film over an unheated grooved plate and a heated grooved plate with its end maintained at elevated temperatures. To investigate the effect of gravity, the grooved surface was placed in upward and downward facing positions. Hydrodynamically controlled and heat conduction controlled rewetting models were presented to explain and predict the rewetting behavior. The following conclusions can be reached: (i) Profound gravitational effects were observed as the rewetting velocity was found to be higher in the upward than in the downward facing orientation, and the difference was even greater with higher initial plate temperature. (ii) The rewetting velocity increases with the initial plate temperature but then decreases with the plate temperature when the plate temperature exceeds it's rewetting temperature. (iii) The rewetting temperature is not constant, but rather varies in the narrow range of 95 C to 104 C for the condition and fluid tested here. (iv) The rewetting of the plate is hydrodynamically controlled when the initial plate temperature is lower than the rewetting temperature. However, it becomes conduction controlled when the initial plate temperature exceeds the rewetting temperature.

FUTURE WORKS

A critical component in the loop design for rewetting experiments under microgravity environment is the coolant feeder. The feeder should be so designed that it is capable of delivering the coolant to one end of the test section without imposing undue pressure or inertial force in the advancing direction of the rewetting front. This is to ensure that ground tests can properly simulate tests in space environment in which rewetting is driven by capillary force only. As suggested by Dr. Platt, the NASA program manager, we are

therefore devoting the remaining of the present project period in the design and testing of the coolant feeder in preparation for future full scale microgravity experiments.

ACKNOWLEDGEMENT

This work is supported by NASA-Lewis, grant No. NAG3-1381. Help received from Drs. J. Platt, S. Jayawardena and B. Singh is gratefully acknowledged.

References

Alario, J., Brown, R., and Kosson, R., 1983, "Monogroove Heat Pipe Development for the Space Constructable Radiator System", Paper No. AIAA-83-1431.

Chan, S. H., and Zhang, W., 1994, "Rewetting Theory and the Dryout Heat Flux of Smooth and Grooved Plates With a Uniform Heating", ASME Journal of Heat Transfer, Vol. 116, pp. 173-179.

Dreyer, M., Delgado, A., and Rath, H. J., 1994 "Capillary Rise of Liquid between Parallel Plates under Microgravity", Journal of Colluid and Interface Science, Vol. 163, pp.158-168.

Duffey, R. B., and Porthouse, D. T. C.,1993 "The Physics of Rewetting in Water Reactor Emergency Core Cooling", Nuclear Engineering and Design, Vol. 25, pp. 379-394.

Ferng, Y. M., Chieng, C. C., and Pan, C., 1991, "Predictions of Rewetting Processes for a Nuclear Fuel Rod Using First Principles Equation", Nuclear Engineering and Design, Vol.126, pp. 189-205.

Grimley, T. A., Mudawwar, I., and Incropera, F. P., 1988, "CHF Enhancement in Flowing Fluorocarbon Liquid Films Using Structured Surfaces and Flow Deflectors", Int. J. Heat Mass Transfer, Vol. 31, No. 1, pp. 55-65.

Kawazi, M., and Westbye, C. J., 1991, "Microgravity Experiments on Two-Phase Flow and Heat Transfer during Qoenching of a Tube and Filling of a Vessel", AICHE symposium series, Vol. 87, pp. 236-243.

Levine, S., Reed, P., and Watson, E. J., 1976, "A Theory of the Rate of Rise of a Liquid in a Capillary", Colloid and Interface Science, Vol. III, pp. 403-419.

Murray, W. D., and Landis, F., 1959, "Numerical and Machine Solutions of Transient Heat-Conduction Problems Involving Melting or Freezing", ASME Journal of Heat Transfer, Vol. 81, pp. 102-106.

Lyon, D. N., Jones, M. C., Ritter, G. L., Chiladakis, C., and Kosky, P. G., 1965, "Peak Nucleate Boiling Fluxes for Liquid Oxygen on a Flat Horizontal Platinum Surface at Boyancies Corresponding to Accelerations Between -0.03 and 1 g_c", Journal of A.I.Ch.E., Vol. 11, pp. 773-?

Merte, H. Jr., and Clark, J. A., 1964, "Boiling Heat Transfer with Cryogenic Fluids at Standard, Fractional, and Near-Zero Gravity" ASME Journal of Heat Transfer, Vol. 86, pp. 351-359.

Peng, X., and Peterson, G., 1991, "Analytical Investigation of the Rewetting Characteristics of Heated Plates With Grooved Surfaces," Presented at the 1991 National Heat Transfer Conference, Paper No. AIAA-91-4004, Minneapolis, MN.

Peng, X., and Peterson, G., 1992, "Analysis of Rewetting for Surface Tension Induced Flow", ASME Journal of Heat Transfer, Vol.114, pp.703-707.

Sun, K. H., Dix, D. E., and Tien, C. L., 1974, "Cooling of a Very Hot Vertical Surface by a Falling Liquid Film", ASME Journal of Heat Transfer, Vol.96, pp. 126-131.

Stroes, G., Fricker, D., Issacci, F., and Catton, I., 1990, "Heat Flux Induced Dryout and Rewet in thin Films", Proc. 9th Int. Heat Trans. Conv., Vol. 6, pp. 359-364.

Thompson, T. S., 1972, "An Analysis of the Wet-Side Heat-Transfer Coefficient During Rewetting of a Hot Dry Patch", Nuclear Engineering and Design, Vol. 22, pp. 212-224.

Tien, C. L., and Yao, L. S., 1975, "Analysis of Conduction-Controlled Rewetting of a Vertical Surface", ASME Journal of Heat Transfer, Vol. 97, pp. 161-165.

Yamanouchi, A., 1968, "Effect of Core Spray Cooling in Transient State After Loss of Cooling Accident", Journal of Nuclear Science and Technology, Vol. 5, pp.547-558.

Nomenclature

A	dimensionless heat source
A_l	liquid cross section n the groove, m^2
A_w	wetted wall area, m^2
B	Biot number with respect to the convective heat transfer coefficient
C_p	thermal capacitance, J/kg·C
h	surface convective heat transfer coefficient, $W/m^2 \cdot C$
K	thermal conductivity, W/m·C
l_1	groove depth, m
l_2	groove land, m
l_3	groove width, m
P	dimensionless rewetting velocity (Peclet number)
q	uniform heat flux, W/m^2
s	rewetting distance, m
s_1	plate thickness, m
T	temperature, C
T_1	initial hot surface temperature, C
T_0	Leidenfrost temperature, C
T_s	liquid saturation temperature, C
t	time, sec
V	rewetting front velocity, m/sec
x	axial length in moving front coordinate, m
x'	axial length in stationary coordinate, m
η	dimensionless length coordinate with respect to x
η'	dimensionless length coordinate with respect to x'
η_{L1}	dimensionless wet region length
η_{L2}	dimensionless dry region length
η_L	dimensionless total length
θ	dimensionless temperature
τ	dimensionless time
ρ	density, kg/m^3

Figures

Fig. 1

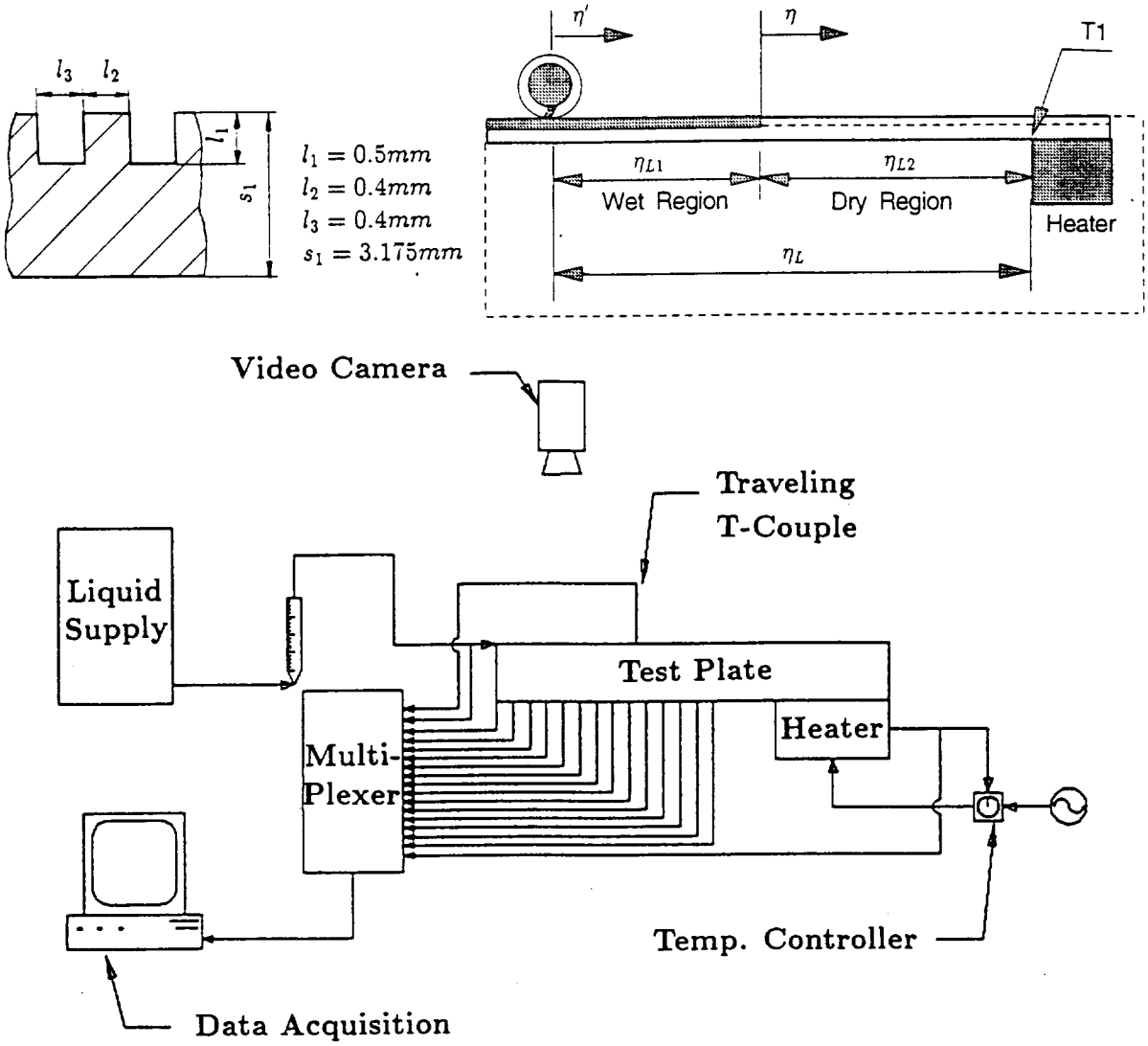
l_3 l_2
l_1
s_1
$l_1 = 0.5mm$
$l_2 = 0.4mm$
$l_3 = 0.4mm$
$s_1 = 3.175mm$
η'
η
T1
η_{L1}
η_{L2}
Wet Region
Dry Region
Heater
η_L
Video Camera
Traveling
T-Couple
Liquid
Supply
Test Plate
Heater
Multi-
Plexer
Temp. Controller
Data Acquisition

Fig. 1

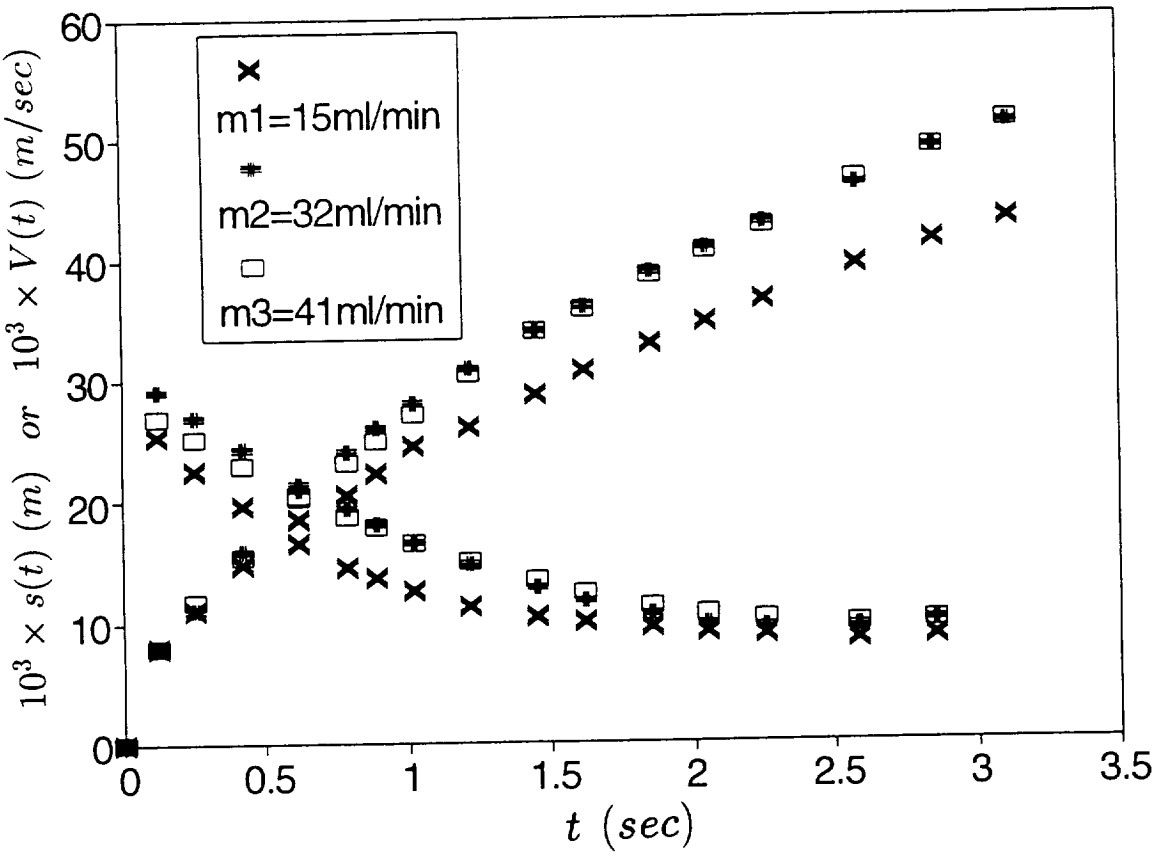

Fig. 2

Flow Rate effect

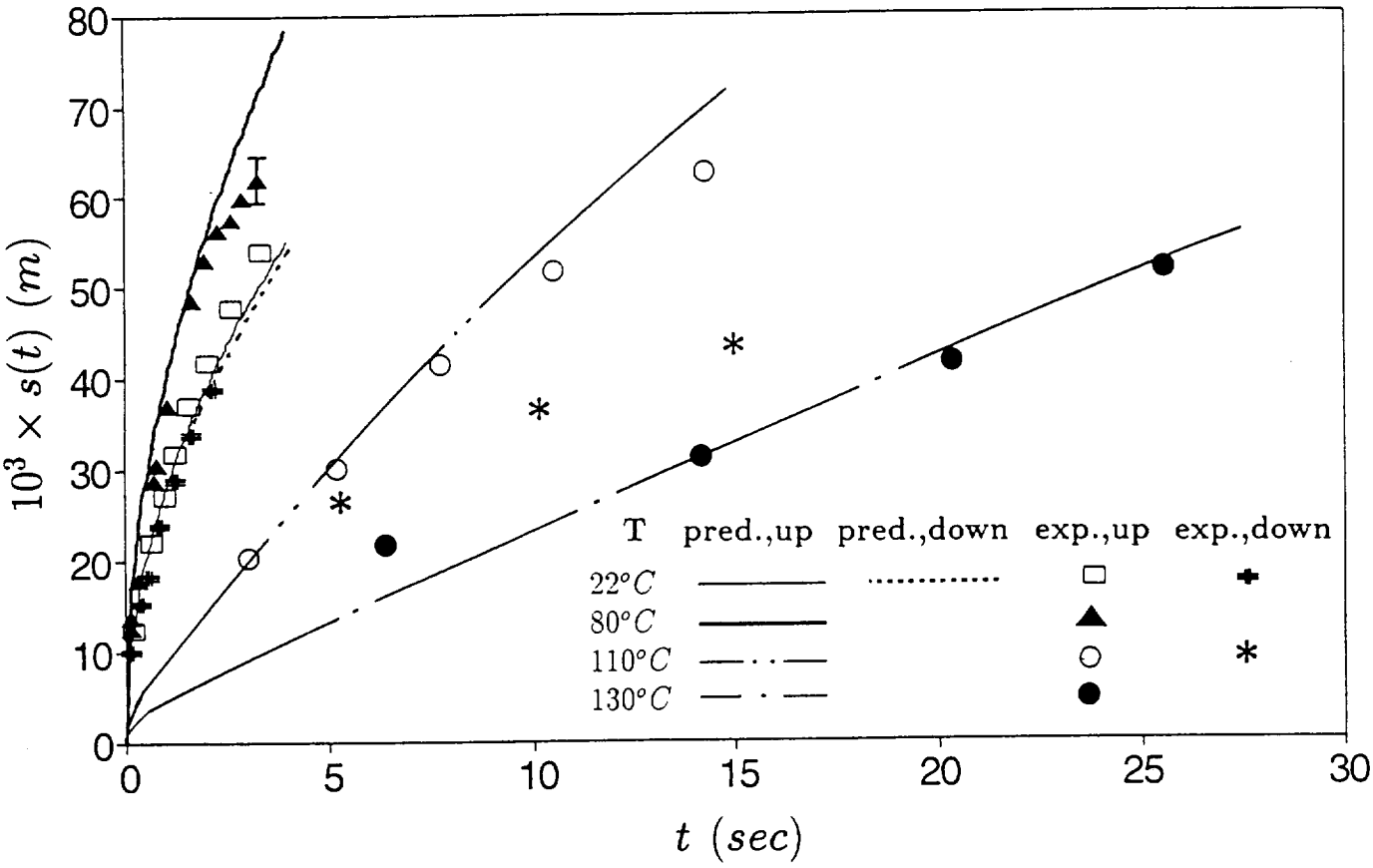
80
70
60
50
40
30
20
10
0
$10^3 \times s(t)\ (m)$
0
5
10
15
20
25
30
$t\ (sec)$
T pred.,up pred.,down exp.,up exp.,down
22°C
80°C
110°C
130°C

Fig. 3

Fig 4

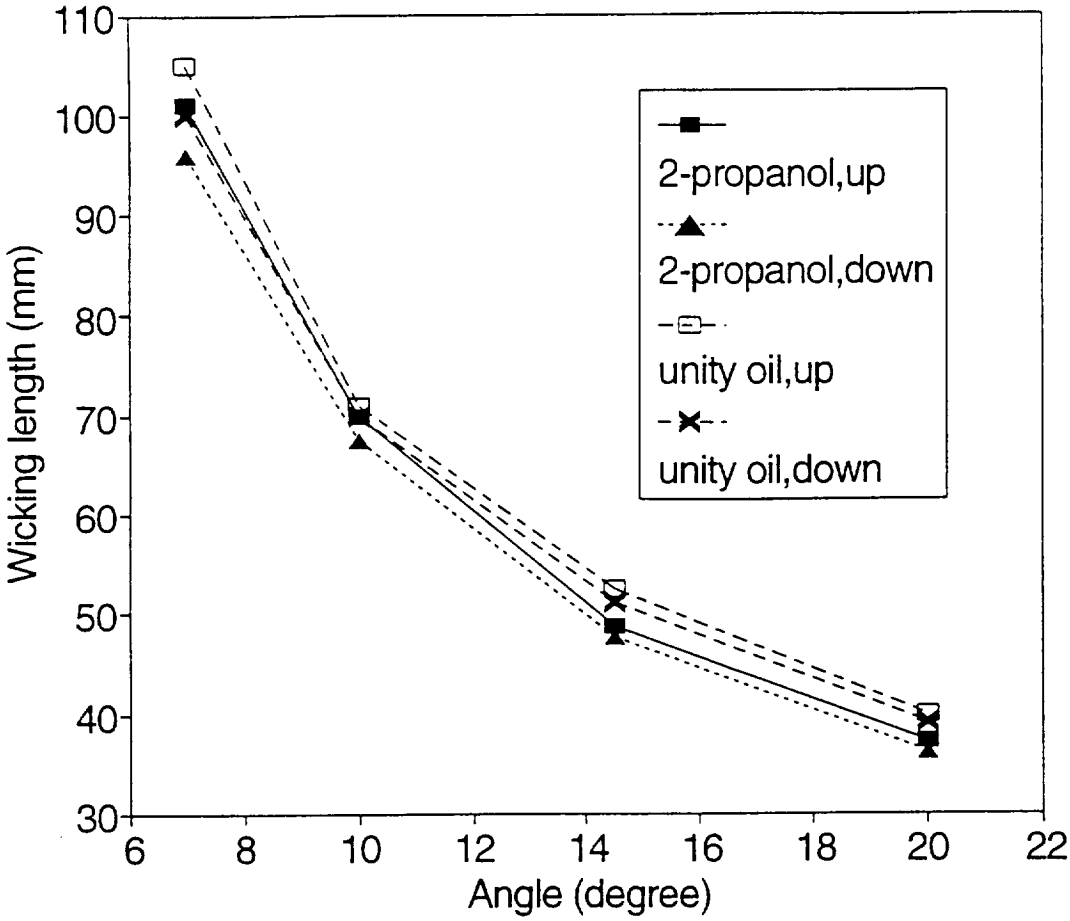
110
100
90
80
70
60
50
40
30
Wicking length (mm)
6
8
10
12
14
16
18
20
22
Angle (degree)
2-propanol,up
2-propanol,down
unity oil,up
unity oil,down

Fig 4

Fig. 5

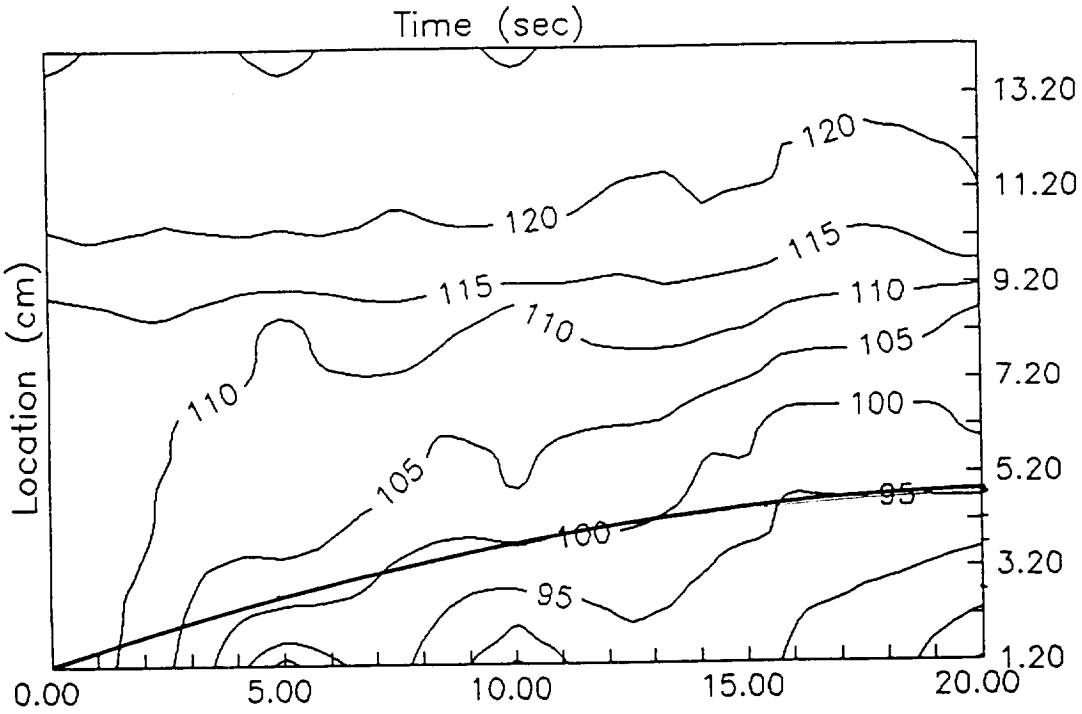
Time (sec)
Location (cm)
13.20
11.20
9.20
7.20
5.20
3.20
1.20
0.00
5.00
10.00
15.00
20.00
120
120
115
115
110
110
105
105
100
100
95
95

Fig. 6

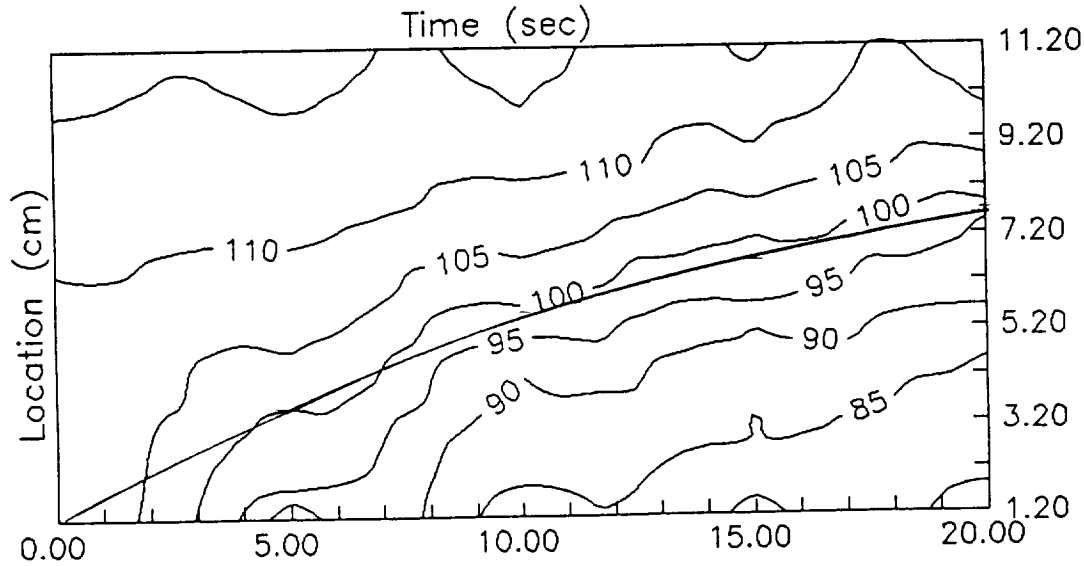
Time (sec)
Location (cm)
11.20
9.20
7.20
5.20
3.20
1.20
0.00
5.00
10.00
15.00
20.00
110
110
105
105
100
100
95
95
90
90
85

Fig. 7

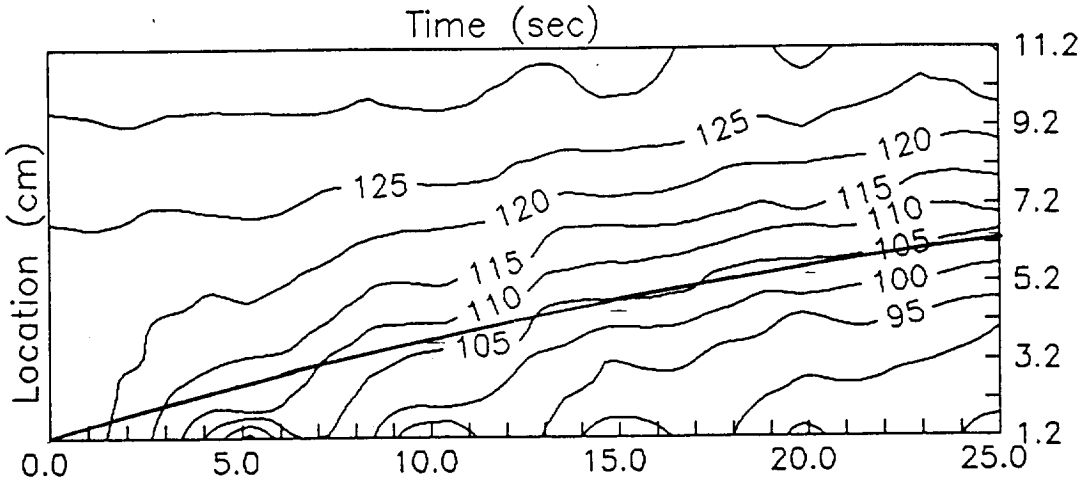
Time (sec)
Location (cm)
0.0
5.0
10.0
15.0
20.0
25.0
1.2
3.2
5.2
7.2
9.2
11.2
125
120
115
110
105
100
95

Fig. 8

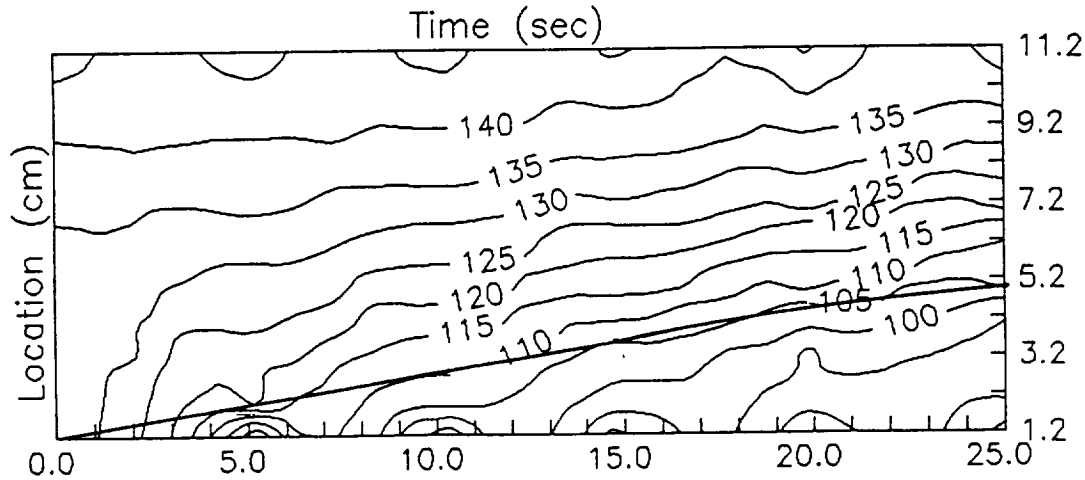
Time (sec)
Location (cm)
0.0
5.0
10.0
15.0
20.0
25.0
1.2
3.2
5.2
7.2
9.2
11.2
140
135
130
125
120
115
110
105
100

Fig 9

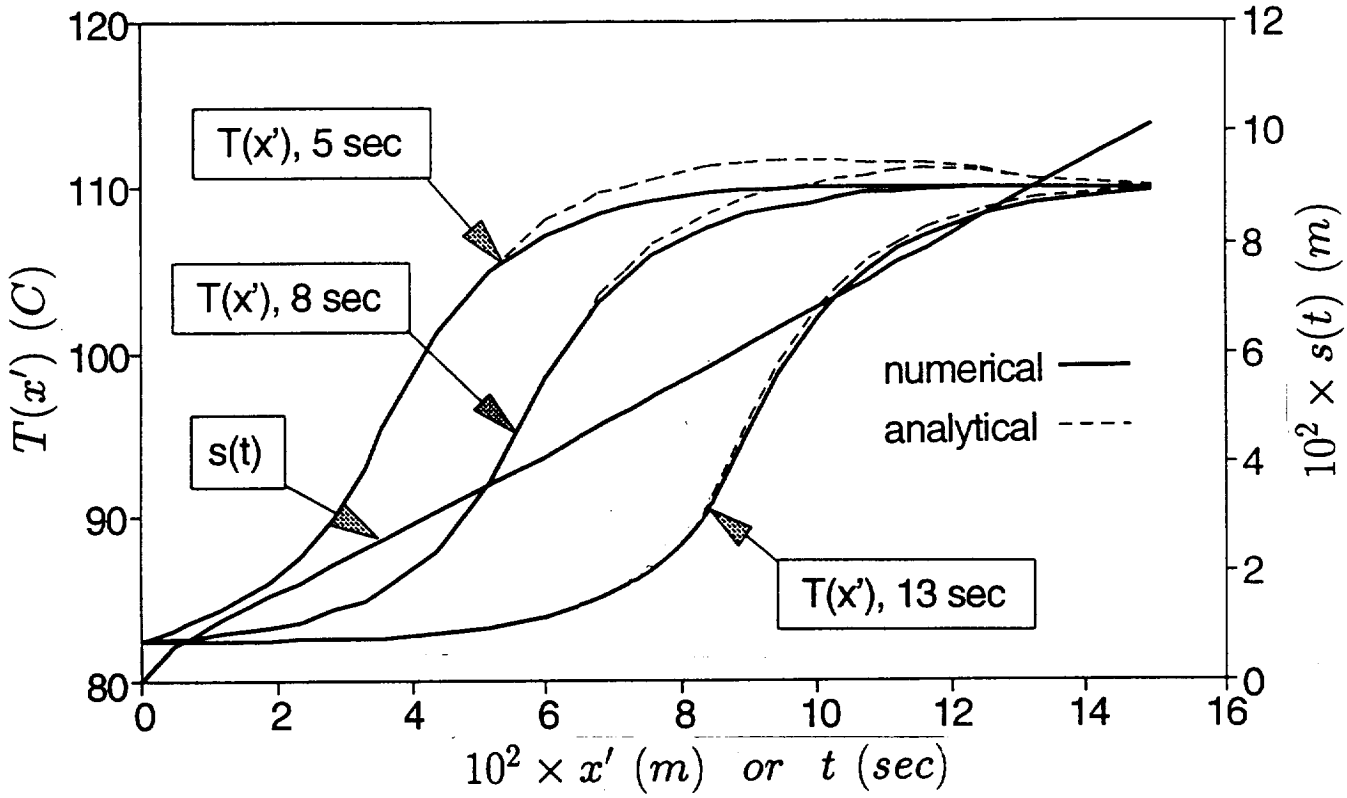
T(x'), 5 sec
T(x'), 8 sec
s(t)
T(x'), 13 sec
numerical
analytical
$T(x')\ (C)$
$10^2 \times s(t)\ (m)$
$10^2 \times x'\ (m)$ or $t\ (sec)$
120
110
100
90
80
12
10
8
6
4
2
0
0
2
4
6
8
10
12
14
16

Fig. 9

Fig. 1°

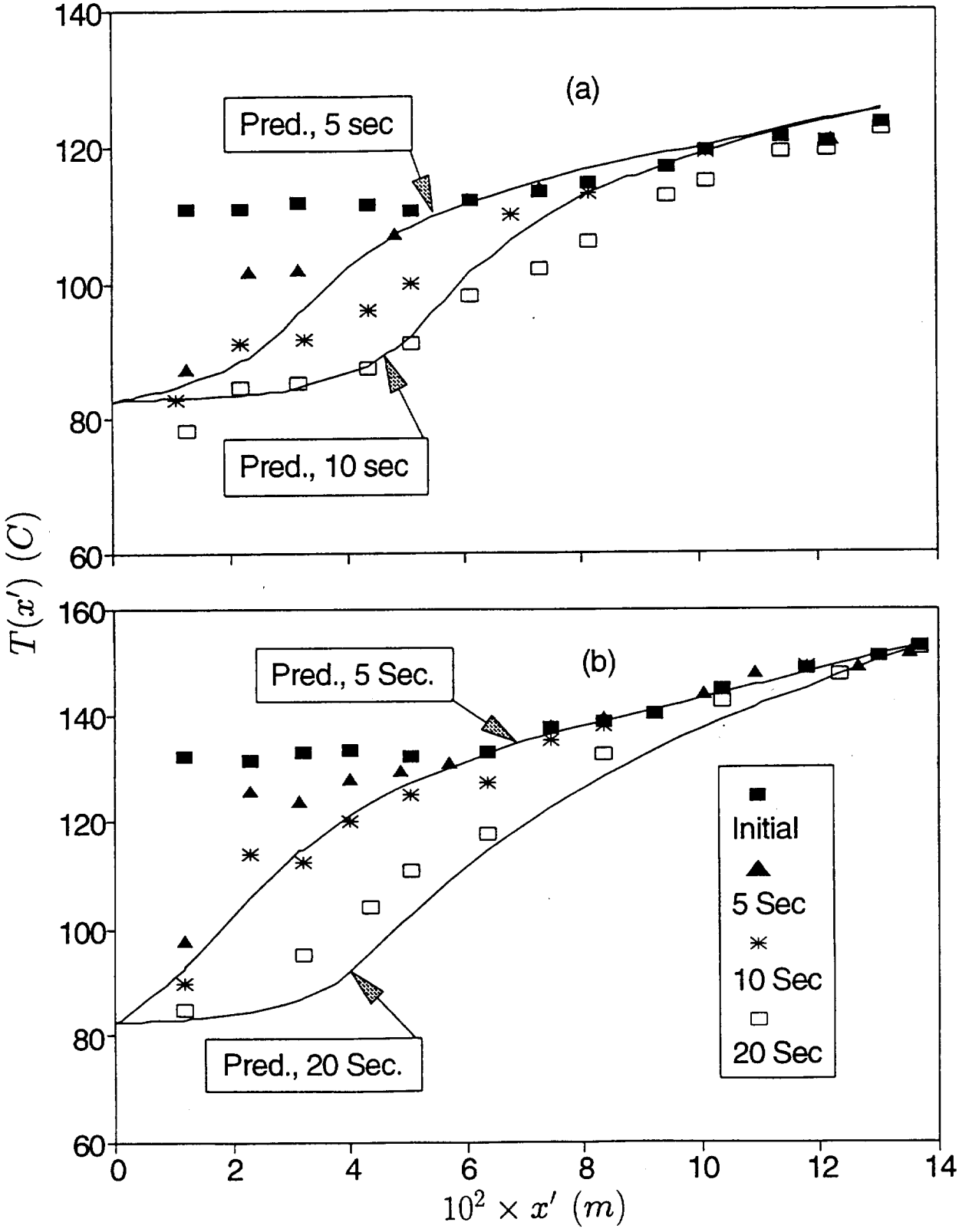
(a)
Pred., 5 sec
Pred., 10 sec
(b)
Pred., 5 Sec.
Pred., 20 Sec.
Initial
5 Sec
10 Sec
20 Sec
$T(x')$ (C)
$10^2 \times x'$ (m)
140
120
100
80
60
160
140
120
100
80
60
0
2
4
6
8
10
12
14

Fig. 10